Appendix. Structural properties and linear transformations in the multidimensional systems with symmetric links

In this Appendix we consider the basic properties of the one class of multidimensional linear systems. This particular class important for design of electronic systems, including operational amplifiers, can be reduced to the systems with two input and two output variables and one common mode feedback. The equivalent structural graphs are presented, and the transfer coefficients for common mode and differential mode components of the input and output signals are derived. These transfer coefficients are also used to evaluate the influence of variations of the structure parameters. Some simple transistor amplifiers with n inputs and n outputs are shown as examples.

1. We consider a special class of multidimensional (multichannel) linear systems with symmetric links that can be represented by a graph of fig. A1a or by equations:

$$z_i = -q_i^{'}(u_i + r_i x_c) \qquad (i = \overline{1,n}) \qquad \text{(A.1)}$$

$$x_c = \rho_c y_c\,; \qquad y_c = \sum_{i=1}^{n} c_i z_i$$

where u_i are input signals, z_i are output signals, c_i, $q_i^{'}$, r_i $(i = \overline{1,n})$ and ρ_c are transfer coefficients. The same transformation of the input vector **u** into output vector **z** may also be represented by the equivalent signal graph in fig. A1b.

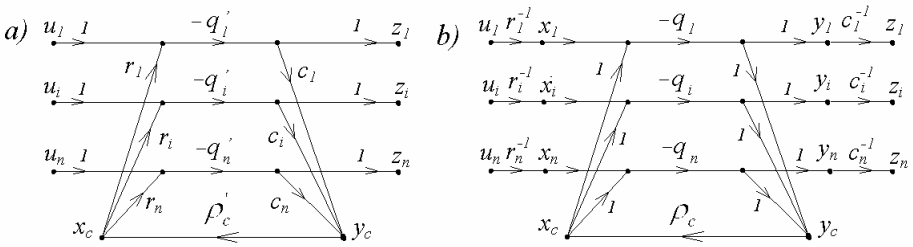

Figure A1. Graph of the multidimensional system with common-mode feedback

In this figure $q_i = r_i q_i^{'} c_i$, and the signals $x_i = r_i^{-1} u_i$ and $y_i = c_i z_i$ $(i = \overline{1,n})$ are inner variables. The systems described by the graphs of fig. A1 may be called the *systems with common mode feedback,* which can be positive or negative.

2. Any channel a out of n can be chosen and the rest of $(n-1)$ channels could be combined in a single channel b. It allows one to limit consideration by the two-dimensional system of fig. A2, where

$$q_b = \sum_{i\neq a}^{n} q_i; \qquad x_b = \frac{1}{q_b}\sum_{i\neq a}^{n} q_i x_i = \frac{1}{q_b}\sum_{i\neq a}^{n} q_i r_i^{-1} u_i; \qquad y_b = \sum_{i\neq a}^{n} c_i^{-1} y_i \tag{A.2}$$

This substitution simplifies the analysis, and, at the same time, helps to visualize, without complicated matrix formalism, the general properties of the system and effects of the variations of the system parameters.

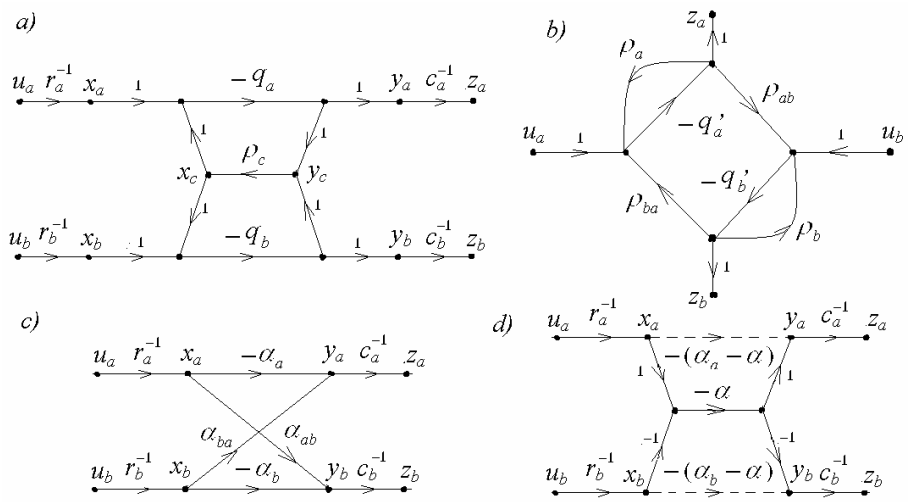

Figure A2. Graph of the two-dimensional system with common-mode feedback

3. The graph of fig. A2a may be transformed in other equivalent forms that may be more convenient for analysis and synthesis of particular electronic systems. The considered two-channel systems can be easily reduced to the equivalent bridge representation (fig. A2b). Signal graphs shown in fig. A2a and A2b are equivalent if

$$\begin{aligned} &\rho_a = r_a\rho_c c_a; \qquad \rho_{ba} = r_a\rho_c c_b; \qquad q_a = r_a q_a' c_a \\ &\rho_{ab} = r_b\rho_c c_a; \qquad \rho_b = r_b\rho_c c_b; \qquad q_b = r_b q_b' c_b \end{aligned} \tag{A.3}$$

From these relationships one can find that

$$\frac{\rho_a}{\rho_{ab}} = \frac{\rho_{ba}}{\rho_b} = \frac{r_a}{r_b}; \qquad \frac{\rho_a}{\rho_{ba}} = \frac{\rho_{ab}}{\rho_b} = \frac{c_a}{c_b} \tag{A.4}$$

The bridge structures have a high sensitivity to variations of feedback parameters that violate the relationships satisfying (A.4), especially when $r_a = r_b = 1$ and/or $c_a = c_b = 1$. This property is routinely used in instrumentation (bridge sensors).

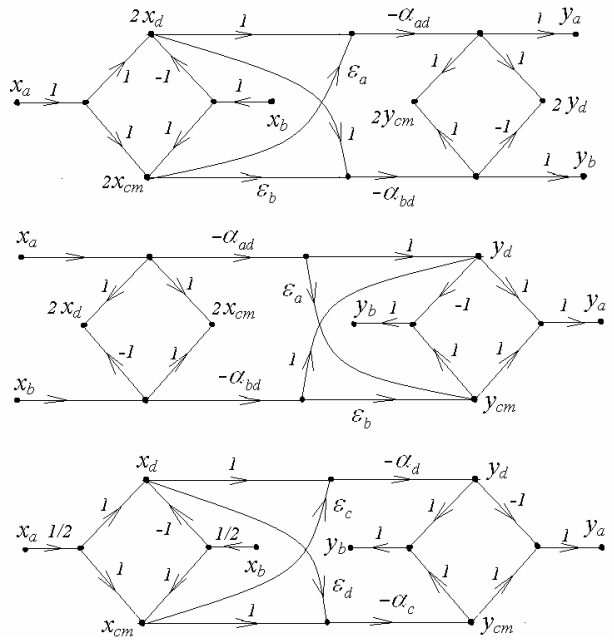

Figure A3. Two-dimensional systems with eliminated feedback

4. Using the rules of signal graph transformations [25] the graph of fig. A1a can be modified into forms without feedback (fig. A2c and d) where:

$$z_a = -c_a^{-1}(\alpha_a r_a^{-1} u_a - \alpha\, r_b^{-1} u_b)$$
$$z_b = -c_b^{-1}(\alpha\, r_a^{-1} u_a - \alpha_b\, r_b^{-1} u_b) \tag{A.5}$$

$$\alpha_a = \frac{q_a(1+\rho_c q_b)}{1+\rho_c(q_a+q_b)}; \qquad \alpha_b = \frac{q_b(1+\rho_c q_a)}{1+\rho_c(q_a+q_b)};$$
$$\alpha_{ab} = \alpha_{ba} = \alpha = \frac{q_a \rho_c q_b}{1+\rho_c(q_a+q_b)}. \tag{A.6}$$

If

$$\rho_c \cdot \min(q_a, q_b) >> 1 \tag{A.7}$$

then the transfer coefficients become

$$\alpha_a = \alpha_b = \alpha = (q_a^{-1} + q_b^{-1})^{-1} = \tilde{q} \tag{A.8}$$

Introducing differential and common mode components of the input signal

$$x_d = (x_a - x_b)/2; \qquad x_{cm} = (x_a + x_b)/2; \tag{A.9}$$

one transforms the graph of fig. A2b into the graph of fig. A-3a. For this graph, one has in the channel a,

$$y_a = -2\alpha_{ad}(x_d + \varepsilon_a x_{cm}) \tag{A.10}$$

where

$$\alpha_{ad} = \frac{1}{2}(\alpha_a + \alpha) = \frac{q_a/2 + \rho_c q_a q_b}{1+\rho_c(q_a+q_b)} \approx \tilde{q}/2 \tag{A.11}$$

is the gain of the differential signal in the channel a, and

$$\varepsilon_a = \frac{\alpha_a - \alpha}{\alpha_a + \alpha} = \frac{1}{1 + 2\rho_c q_b} \tag{A.12}$$

is the attenuation of the common mode signal in the channel a. For channel b

$$y_b = -2\alpha_{bd}(x_d + \varepsilon_b x_{cm}) \tag{A.13}$$

and, substituting b instead of a and changing signs, one can find similar to (A.11) and (A.12) expressions for the differential gain, α_{bd}, and common mode attenuation, ε_b, in the channel b.

The same parameters ε_a, ε_b, α_{ad}, α_{bd} define the dependence of the differential output signal $y_d = (y_a - y_b)/2$ and common mode signal $y_{cm} = (y_a + y_b)/2$ as a function of the variable x_a (graph of fig. A-3b):

$$(y_d)_a = -\alpha_{ad} x_a; \qquad (y_{cm})_a = -\varepsilon_a (y_d)_a \tag{A.14}$$

or as a function of x_b:

$$(y_d)_b = -\alpha_{bd} x_b; \qquad (y_{cm})_b = -\varepsilon_b (y_d)_b \tag{A.15}$$

One can also find the dependencies of the differential, y_d, and common mode, y_{cm}, components from x_d and x_{cm} (graph of fig. A3c). After simple substitutions one obtains that

$$\begin{aligned} y_d &= -\alpha_d (x_d + \varepsilon_c x_{cm}); \\ y_{cm} &= -\alpha_c (\varepsilon_d x_d + x_{cm}), \end{aligned} \tag{A.16}$$

where

$$\begin{aligned} \alpha_d &= \alpha_{ad} - \alpha_{bd} = \frac{2\rho_c q_a q_b + (q_a + q_b)/2}{1 + \rho_c (q_a + q_b)}; \\ \varepsilon_c &= \frac{\alpha_a - \alpha_b}{\alpha_{ad} - \alpha_{bd}} = \frac{(q_a - q_b)}{(q_a + q_b) + 4\rho_c q_a q_b}; \end{aligned} \tag{A.17}$$

and

$$\begin{aligned} \alpha_c &= \frac{\alpha_a + \alpha_b}{2} - \alpha = \frac{(1/2)(q_a + q_b)}{1 + \rho_c (q_a + q_b)} \approx \frac{1}{2\rho_c}; \\ \varepsilon_d &= \frac{\alpha_a - \alpha_b}{\alpha_a + \alpha_b - 2\alpha} = \frac{q_a - q_b}{q_a + q_b}. \end{aligned} \tag{A.18}$$

The equations (A.10)-(A.18), and the corresponding graphs of fig. A3 represent different cases useful in design of instrumentation and amplification systems.

5. When the left side in (A.7) increases the attenuation of the common mode components x_{cm} and y_{cm} also increases. This allows one to amplify even very small differential signal x_d and to resolve very small difference y_d or to obtain the signal proportional to a very small difference of two parameters:

$$2x_d = u_0 (r_a^{-1} - r_b^{-1}); \qquad y_d = y_0 (c_a^{-1} - c_b^{-1}), \tag{A.19}$$

and $u_a = u_b = u_0$ or $y_a = y_b = y_0$ even if the channel gains are different, i.e. $q_a \neq q_b$.

If, in addition to (A.7), the gain of one channel is much larger than the gain of another one, for example,

$$q_b >> q_a \text{ then } \tilde{q} \to q_a. \tag{A.20}$$

Also, as follows from (A.6) and (A.10):

$$\alpha \approx \alpha_a \approx \alpha_b \approx \tilde{q} \approx q_a \tag{A.21}$$

The condition (A.20) may occur if the channel a has a local feedback, or the gain of this channel has changed due to nonlinear distortions or variation of bias with time. It may also occur if the channel b represents the equivalent of $(n-1)$ channels in the n -channel system and

$$q_b = \sum_{i \neq a}^{n} q_i \approx (n-1)q >> q_a \qquad \text{(A.22)}$$

The n two-channel systems that obtained from a single n -channel system by choosing one channel as a -channel and grouping all other channels into b -channel may have different transmissions α_a ($a = \overline{1,n}$) for the differential mode signal $(x_a - x_b)/2$. Yet, the attenuation parameters of the common mode signal $\varepsilon_a = (2\rho_c q_b)^{-1}$ and $\varepsilon_b = (2\rho_c q_a)^{-1}$ at the input and output of each pair of channels may be very small if the condition (A.7) is satisfied.

6. The two-channel structure of fig. A-2 may be interpreted as a general structure of a control system where q_b , r_b , c_b are transfer coefficients of the controlled object, its input sensors and the output transducers, and q_a , r_a , c_a are transfer coefficients of the model representing desirable properties. The parameter ρ_c represents the feedback amplifier amplifying the difference between the outputs of the object and the model.

For example, one can consider as a model the compensation unit included in the feedback link (fig. A-4a) or in the feedforward link (fig. A-4b).

If the inequalities A.7 and A.20 are valid, and $r_a^{-1} >> r_b^{-1}$ (see fig. A-2a) then the outputs of the object and the model, as it follows from A.4, are approximately equal, i.e.

$$y_a \approx c_a z_a \approx y_b \approx c_b z_b \approx q_a r_a^{-1} u_a \qquad \text{(A.23)}$$

and defined by the parameters q_a , r_a and the control signal u_a of the model.

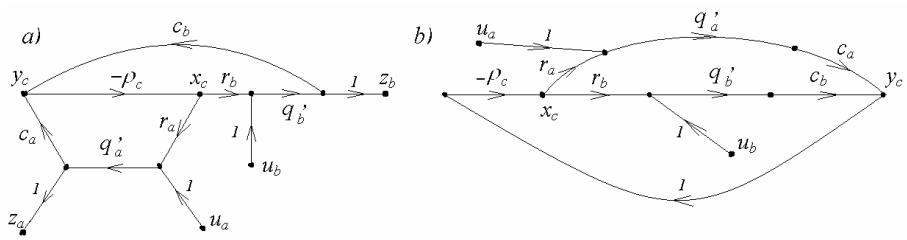

Figure A4. Systems with models

These properties are preserved for any dimension n_b of the object ($n_a + n_b = n$, $n_a >> n_b$). The relationships A.9 - A.15 allow one to evaluate the degree of independence of the control system parameters on the object properties.

7. If one changes the sign of the link transfer in channel a or in feedback as shown in fig. A-5a ($r_a, c_a, \rho_{ab}, \rho_{ba} < 0$) then the common-mode feedback suppresses the differential (and not the common-mode as before) component of the input and output signals. In other words,

the parametric differences between channels as well as the difference between input signals due to different biasing, noise, etc. are reduced in this system.

All previous relationships are valid for this structure as well, but $\varepsilon, \varepsilon_a, \varepsilon_b$ now mean attenuation of the differences while $\alpha_{ad}, \alpha_{bd}, \alpha_d$ are now the transfer coefficients of the common-mode signals.

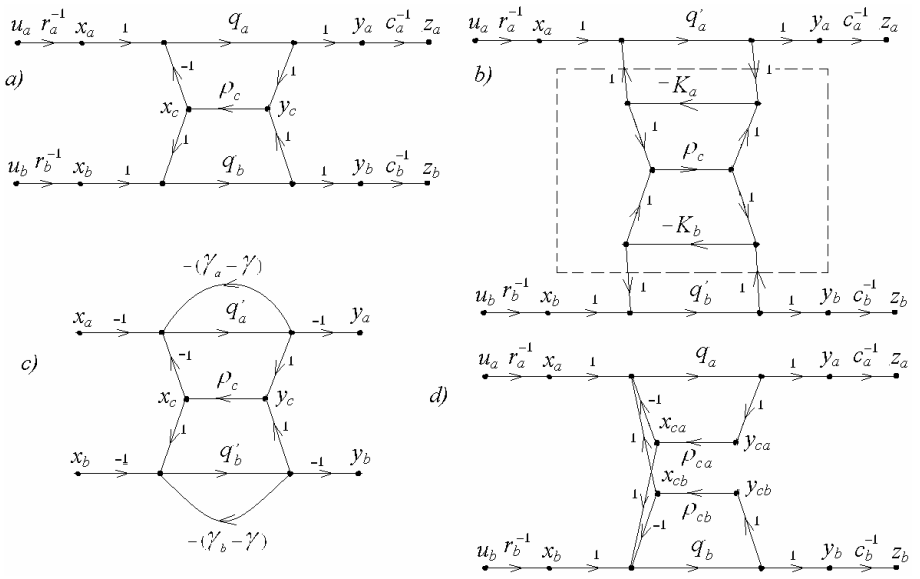

Figure A5. Useful modifications of two-dimensional system graph

8. Some other useful modifications of the general structure are shown in fig. A5b and A5c. The figure A-5b highlights the fact that the common-mode feedback link in the general structure of fig. A-2a can also have, in turn, the same structure. It can also be seen as if each of the links q_a', q_b' has its own local feedback but the parameters of these feedbacks are defined by the main common-mode link.

The signal inversions can be implemented at the input links and the units q_a', q_b' can have their own local feedback links $-(\gamma_a - \gamma)$ and $-(\gamma_b - \gamma)$ as shown in fig. A-5c. The resulting link transfers are:

$$q_a = \frac{q_a'}{1+(\gamma_a - \gamma)q_a'} \text{ and } q_b = \frac{q_b'}{1+(\gamma_b - \gamma)q_b'} \tag{A.24}$$

If the condition (A.7) is satisfied for this structure, and the structure is changed to the form without feedbacks as in fig. A-2d, then

$$\alpha = \frac{q_a q_b \gamma}{1+\gamma(q_a + q_b)} \approx (\frac{1}{q_a} + \frac{1}{q_b})^{-1} \approx (\frac{1}{q_a'} + \frac{1}{q_b'} + \frac{1}{\rho_c}) \tag{A.25}$$

Other relationships for this structure can be derived in the same way as A.8 – A.18.

The fig. A-2a common mode feedback link can also be split in two links. This creates the equivalent structure shown in fig. A-5d. Here each of $q_a^{'}, q_b^{'}$ links has its own feedback, and these feedbacks affect also the opposite signal paths.

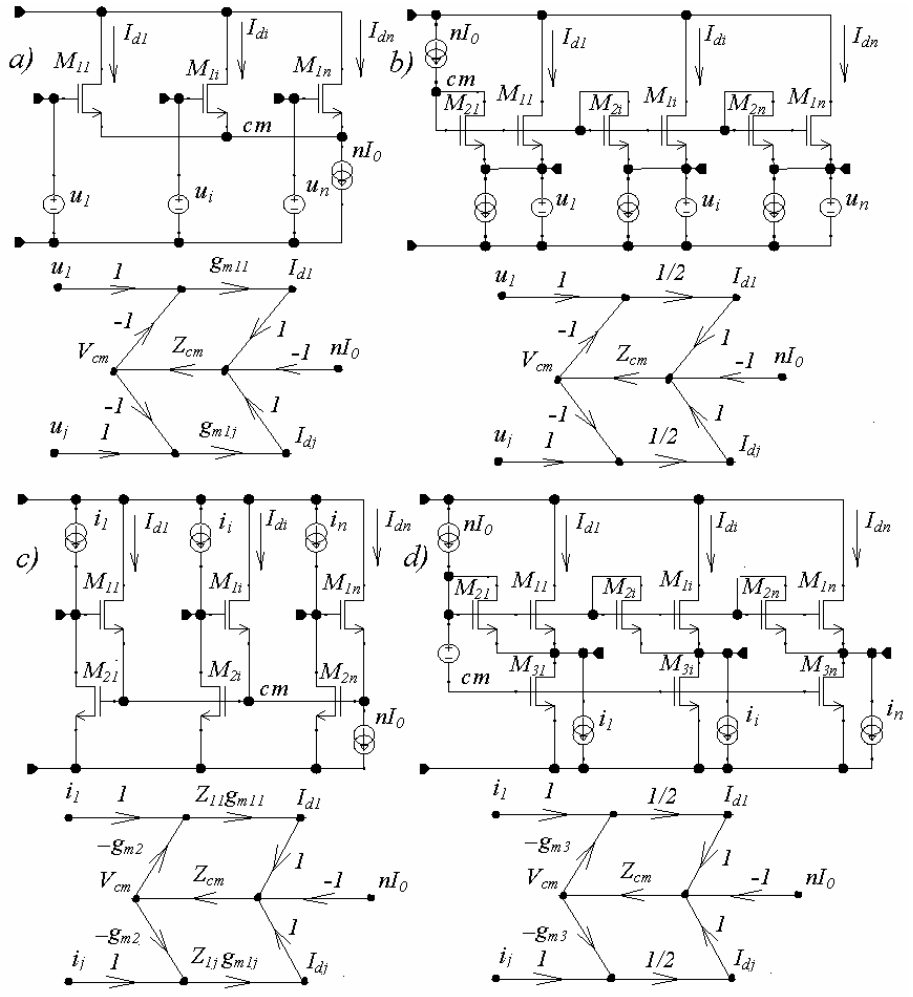

Figure A-6. Four types of input stages

9. With addition of the cross links at input and output, the general structure with common-mode feedback can be considered as functionally complete unit for implementation of linear multidimensional systems (in the same sense as NOR and NAND cells are functionally complete for logic operations). For example, it can be used to represent voltage and current relationships in arbitrary electrical networks.

Table A1 shows three types of summing circuits for current or voltage signal sources having a common load. The complementary distributing circuits of the signal from the

common source between loads are shown in Table A2. All these circuits can be described by the same graph with common-mode feedback as shown in the bottom row of the tables. The choice of the input and output variables in the graph defines the type of the circuit it represents.

10. The differential input stages of the voltage and current amplifiers can also be reduced to the general structure as shown in fig. A6. Fig. A6a represents the voltage controlled current sources (large output impedances, high input impedances). The output current of each source depends on the difference between the input voltage of this source and the average input voltage, namely

$$I_i - I_0 = g_{mi}(u_i - \overline{u}) \; ; \; \overline{u} = \frac{1}{n}\sum_{i=1}^{n} u_i \quad i = \overline{1,n} \tag{A.26}$$

The same structure may represent a completely different stage of fig. A6b. This stage has a large common-mode and small differential input resistance. The input resistance of each channel is equal to $1/g_{mi}$, yet, the output currents are expressed by equation (A.26).

The input stage with large differential and small common-mode input impedance is shown in fig. A-6c. The input stage where both low differential and common mode impedances are low is shown in fig. A-6d.

Numerous implementations of these stages are possible depending on the component cell library at hand.

11. The differential structure with common-mode feedback can model very wide variety of multidimensional systems. This structure helps to understand the common properties and differences of these systems, and, which is the most important, to synthesize the circuits with desired properties.

Table AA1. Summing circuits using passive components

	Current	Voltage	Application
Simple summing	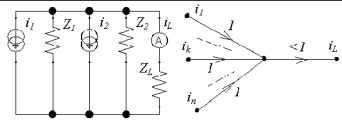 $i_L = (1+\sum_{k=1}^{n} G_k^{-1})^{-1} \sum_{k=1}^{n} i_k =$ $= \sum_{k=1}^{n} i_k$ if $\sum_{k=1}^{n} \left\| G_k^{-1} \right\| << 1$ and $z_L \to 0$	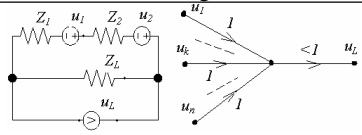 $u_L = (1+\sum_{k=1}^{n} G_k)^{-1} \sum_{k=1}^{n} u_k =$ $= \sum_{k=1}^{n} u_k$ if $\sum_{k=1}^{n} \left\| G_k \right\| << 1$ and $z_L \to \infty$	Power circuits with ideal sources Feedback circuits with ideal instrument
Weighted summing	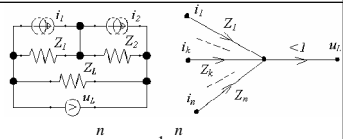 $u_L = (1+\sum_{k=1}^{n} G_k)^{-1} \sum_{k=1}^{n} z_k i_k \approx$ $\approx \sum_{k=1}^{n} z_k i_k$ if $\sum_{k=1}^{n} \left\| G_k \right\| << 1$ and $z_L \to \infty$	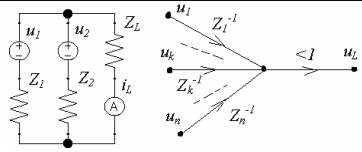 $i_L = (1+\sum_{k=1}^{n} G_k^{-1})^{-1} \sum_{k=1}^{n} i_k =$ $= \sum_{k=1}^{n} i_k$ if $\sum_{k=1}^{n} \left\| G_k^{-1} \right\| << 1$ and $z_L \to 0$	Low power circuits, only with ideal instrument
Averaging summing	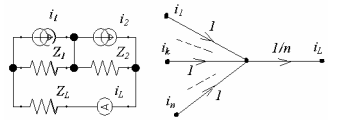 $i_L = \frac{\sum_{k=1}^{n} G_k^{-1} i_k}{\sum_{k=1}^{n} G_k^{-1} + 1} \approx \frac{\sum_{k=1}^{n} z_k^{-1} i_k}{\sum_{k=1}^{n} z_k^{-1}}$ $i_L = \frac{1}{n} \sum_{k=1}^{n} i_k$ if $z_k = z_0$	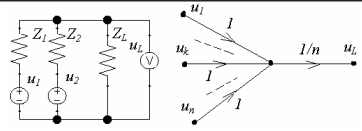 $u_L = \frac{\sum_{k=1}^{n} G_k u_k}{\sum_{k=1}^{n} G_k + 1} \approx \frac{\sum_{k=1}^{n} z_k^{-1} u_k}{\sum_{k=1}^{n} z_k^{-1}}$ $u_L = \frac{1}{n} \sum_{k=1}^{n} u_k$ if all $z_k = const = z_0$	Low power circuits with ideal instrument Power circuits if $G_k = G_0$
Summing circuit graph	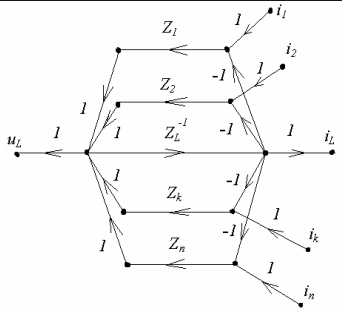	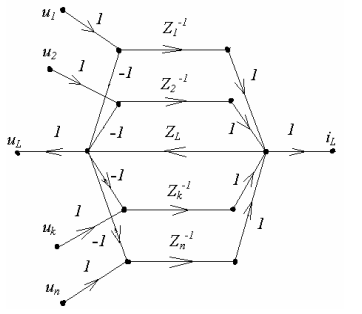	

Notes. 1. Ideal current instrument $z_i \to 0$; ideal voltage instrument $z_i \to \infty$; ideal voltage source $z_i \to 0$; ideal current source $z_i \to \infty$.

2. $G_k = z_L^{-1} z_k$, $k = \overline{(1,n)}$; $G_k^{-1} = z_L z_k^{-1}$.

Table AA2. Distributing circuits using passive components

	Voltage	Current	Application
Simple distributing	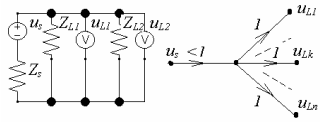 $u_{Lk} = (1+\sum_{k=1}^{n} G_k)^{-1} u_s \approx u_s$ if $\sum_{k=1}^{n} \lvert G_k \rvert >> 1$ and $z_s \to 0$	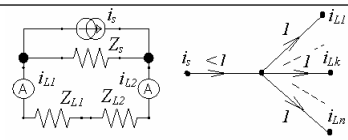 $i_{Lk} = (1+\sum_{k=1}^{n} G_k^{-1})^{-1} i_s \approx i_s$ if $\sum_{k=1}^{n} \lvert G_k^{-1} \rvert >> 1$ and $z_s \to \infty$	Power circuits with ideal source Measurements with ideal instruments
Weighted distributing	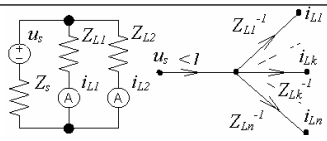 $i_{Lk} = z_{Lk}^{-1}(1+\sum_{k=1}^{n} G_k^{-1})^{-1} u_s \approx z_{Lk} i_s$ if $\sum_{k=1}^{n} \lvert G_k^{-1} \rvert >> 1$ and $z_s \to 0$	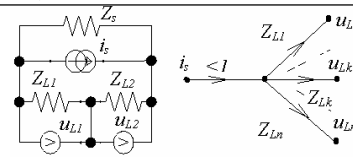 $u_{Lk} = z_{Lk}(1+\sum_{k=1}^{n} G_k)^{-1} i_s \approx z_{Lk} i_s$ if $\sum_{k=1}^{n} \lvert G_k \rvert >> 1$ and $z_s \to \infty$	Input circuits with ideal instruments or sources
Averaging distributing	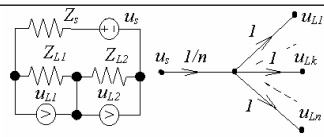 $u_{Lk} = \frac{G_k^{-1} u_s}{1+\sum_{k=1}^{n} G_k^{-1}} \approx \frac{G_k^{-1} u_s}{\sum_{k=1}^{n} G_k^{-1}} \approx \frac{u_s}{n}$ if $\sum_{k=1}^{n} \lvert G_k^{-1} \rvert >> 1$; $z_{Lk} = z_0$	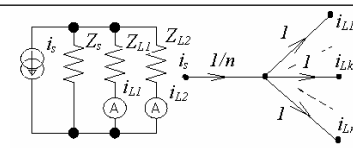 $i_{Lk} = \frac{G_k i_s}{1+\sum_{k=1}^{n} G_k} \approx \frac{G_k i_s}{\sum_{k=1}^{n} G_k} \approx \frac{i_s}{n}$ if $\sum_{k=1}^{n} \lvert G_k \rvert >> 1$; $z_{Lk} = z_0$	Input circuits with ideal sources
Distributor graph	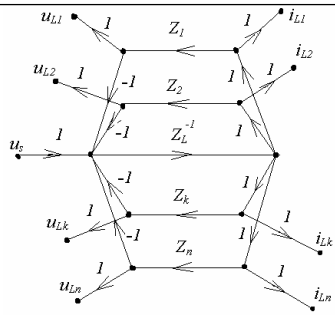	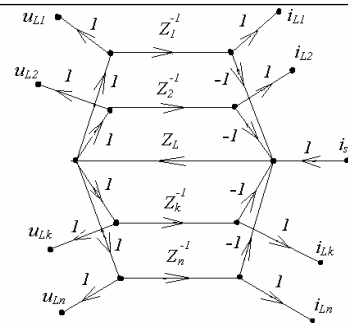	

Notes. 1. Ideal current instrument $z_i \to 0$; ideal voltage instrument $z_i \to \infty$; ideal voltage source $z_s \to 0$; ideal current source $z_s \to \infty$.

2. $G_k = z_{Lk}^{-1} z_s$, $k = (\overline{1,n})$; $G_k^{-1} = z_{Lk} z_s^{-1}$.

References

1. B.D.H. Tellegen ”La recherche pour une serie complete d’elements de circuit ideaux non-lineares”, *Rendiconti Del Seminario Matematico e Fisico di Milano*, vol. 25, pp. 134-144, April 1954.
2. E. Charbon, R. Gharpurey, P. Miliozzi, R. Meyer, and A. Sangiovanni-Vincentelli, *Substrate noise: analysis and optimization for IC design*, Dordreht, The Netherlands: Kluwer, 2001.
3. F. Fruett, and G.C.M. Meijer *The piezojunction effect in silicon integrated circuits and sensors*, Dordrecht, The Netherlands: Kluwer, 2002
4. A. Andreini, C. Contiero, and P. Galbiati, “BCD technology for smart power ICs”, in *Smart Power ICs : technologies and applications*, B. Murari, F. Bertotti, and G.A. Vignola, eds., New York: Springer, 1996.
5. W. Bakalski et al., “A Monolithic 2.45GHz Power Amplifier in SiGe-Bipolar with 0.4W Output Power and 53% PAE at 2V”, *Proc. ESSCIRC-2002*, pp. 223-226, Florence, Italy, Sept. 24-26, 2002.
6. C. Contiero, A. Andreini, and P. Galbiati, “Roadmap Differentiation and Emerging Trends in BCD Technology”, *Proc. ESSDERC-2002*, pp. 275-282, Florence, Italy, Sept. 24-26, 2002.
7. M. Berkhout, “A class D output stage with zero dead time”, *Proc. ISSCC-2003 Digest Tech. Papers*, pp. 1-8, San Francisco, Feb. 9-13, 2003.
8. M. C. Wilson et al., “A 12Volt, 12GHz Complementary Bipolar Technology for High Frequency Analogue Applications”, *Proc. ESSDERC-2002*, pp. 375-378, Florence, Italy, Sept. 24-26, 2002.
9. P. Gray, and R. Meyer, *Analysis and design of analog integrated circuits*, New York: Wiley, 1993.
10. J. H. Huijsing, *Operational amplifiers*, Dordrecht, The Netherlands: Kluwer, 2001.
11. J. Williams, ed., *Analog circuit design*, Oxford, England: Butterworth-Heinemann, 1991.
12. J. O’Connor, and I. McDermott, *The art of systems thinking,* Thorsons, 1997.
13. D. Jones, and K. Martin, *Analog integrated circuit design*, New York: Wiley, 1997.
14. V. Ivanov, and S. Zhang “250 MHz CMOS Rail-to-Rail IO OpAmp”, *Proc. ESSCIRC-2002*, pp. 183-186, Florence, Italy, Sept. 24-26, 2002.

15. V. Ivanov, W. Meinel, and J. Zhou, "Method and circuit for trimming offset and temperature drift for operational amplifiers and voltage references", US pat. 6,614,305, 2003
16. A. Tang, "A 3uV-Offset Operational Amplifier with 20 nV/$\sqrt{Hz}$ Input Noise PSD at DC Employing both Chopping and Autozeroing", *ISSCC-2002 Digest Tech. Papers*, vol. 1, pp. 386-387, San Francisco, Feb. 3-7, 2002.
17. G. M. Weinberg, *An Introduction to General Systems Thinking*, New York: Dorset House, 2001
18. G. Altshuller, *And Suddenly the Inventor Appeared*, Worcester, MA: Technical Innovation Center, Inc., 1996.
19. G. Polya, *How to solve it*, Princeton University Press, 1971.
20. В. Н. Иванов "Динамически-эквивалентные системы", *Чувствительность систем управления*, т. 3, стр. 296-304, Владивосток, 1975, (V. N. Ivanov, "Dynamically equivalent systems", in *Control systems sensitivity,* vol. 3, pp. 296-304, Vladivostok, 1975, in Russian).
21. В.Н. Иванов "Принципы построения мажоритарных систем управления", *Технические средства автоматики*, Москва: Наука, 1971 (V.N. Ivanov "Design principles of the control systems with voting", in *Technical means of automatics*, Moscow: Nauka Pub. House, 1971, in Russian).
22. R. Eschausier, and J. Huijsing, *Frequency compensation techniques for low-power operational amplifiers*, Dordrecht, The Netherlands: Kluwer, 1997.
23. A. Ochoa, "A systematic approach to the analysis of general and feedback circuits and systems using signal flow graphs and driving point impedance" ", *IEEE Trans. Circuits and Systems*, Part II, vol. 45, no. 2, pp. 187–195, Feb. 1998.
24. H. Schmid, "Circuit transposition using signal-flow graphs", *Proc. ISCAS-2002*, vol. 2, pp. 25-28, Phoenix, AZ, May 26-29, 2002.
25. S. Mason, "Feedback theory—Further properties of signal flow graphs", *Proc. IRE*, vol. 44, no. 7, pp. 920–926, July 1956.
26. B. Thandri, and J. Silva-Martínez, "A Robust Feedforward Compensation Scheme for Multistage Operational Transconductance Amplifiers With No Miller Capacitors", *IEEE J. Solid-State Circuits*, vol. SC-38, no. 2, pp. 237-243, Feb. 2003.
27. V. Ivanov, "High-gain amplifier with multipath forward feeding for frequency compensation" US pat. 5,917,376, 1998.
28. W.-H. Ki "Signal Flow Graph Analysis of Feedback Amplifiers", *IEEE Trans. Circuits and Systems*, Part I, vol. 47, no. 6, pp. 926-933, June 2000.
29. *Exar Inc. product catalog*, 1985.
30. E. Seevinck, *Analysis and synthesis of translinear integrated circuits*, New York: Elsevier, 1988.
31. B. Minch, "A low-voltage MOS cascode bias circuit for all current levels", *Proc. ISCAS-2002*, vol. 3, pp. 619-622, Phoenix, AZ, May 26-29, 2002.
32. E. Seevinck, "CMOS translinear circuits" in *Analog Circuit Design*, Dordrecht, The Netherlands: Kluwer, pp. 323-336, 1996.
33. G. F. Olson, *Dynamic analogies*, Princeton, NJ: Van Nostrand, 1958.
34. J. Steininger, "Understanding of the wide-band MOS transistors", *IEEE Circuits and Devices Magazine*, vol. 6, no. 3, pp. 26 –31, May 1990.
35. S. Sanchez, V. Ivanov, and G. Johnson, "Rail-to-rail class AB output stage of the operational amplifier with wide supply range", US pat. 6,545,538, 2003.
36. B. Hosticka et al., "Design methodology for analog monolithic circuits", *IEEE Trans. Circuits and Systems*, Part I, vol. 41, no. 5, pp. 387-394, May 1994.

37. B. Hosticka et al., “CMOS operational amplifier with nearly constant settling time”, *Proc. IEE*, Part G, vol. 137, no. 4, pp. 309-314, Aug. 1990.
38. K. Bult, and G. Geelen “A fast-settling CMOS OpAmp for SC circuits with 90 dB DC gain”, *IEEE J. Solid-State Circuits*, vol. SC-25, no. 6, pp. 1379-1384, Dec. 1990.
39. *OPA363 data sheet and application notes*, *www.ti.com*.
40. A. Boni, "Op-Amps and Startup Circuits for CMOS Bandgap References With Near 1-V Supply", *IEEE J. Solid-State Circuits*, vol. SC-37, no. 10, pp. 1339-1343, Oct. 2002.
41. W. M. Leach, “On the application of the Thevenin and Norton equivalent circuits and signal flow graphs to the small-signal analysis of active circuits”, *IEEE Trans. Circuits and Systems*, Part I, vol. 43, no. 11, pp. 885-893, Nov. 1996.
42. R. D. Kelly, “Electronic circuit analysis and design by driving-point impedance techniques”, *IEEE Trans. Education*, vol. E-13, pp.154-167, Sept. 1970.
43. Y. Hu, and M. Sawan, “A 900 mV high PSRR CMOS voltage reference dedicated to implantable micro-devices”, *Proc. ISCAS-2003*, vol. 1, pp. 373-376, 25-28 May, Bangkok, Thailand, 2003.
44. V. Ivanov, and D. Baum “A 3A 20 MHz BiCMOS/DMOS power operational amplifier: structural design approach”, *ISSCC-2003 Digest Tech. Papers*, pp. 1-10, San-Francisco, Feb. 9-13, 2003.
45. K. de Langen, and J. Huijsing, *Compact low-voltage and high-speed CMOS, BiCMOS and bipolar operational amplifiers*, Dordrecht, The Netherlands: Kluwer, 1999.
46. J. Harrison, and N. Weste, “A 500 MHz anti-alias filter using feed-forward OpAmps with local common-mode feedback”, *ISSCC-2003 Digest Tech. Papers*, pp. 1-9, San-Francisco, Feb. 9-13, 2003.
47. B. Kamath, R. Meyer, and P.Gray “Relationship between frequency response and settling time of operational amplifiers”, *IEEE J. Solid-State Circuits*, vol. SC-9, no. 6, pp. 347-352, Dec. 1974.
48. *OPA620 data sheet and application notes*, *www.ti.com*
49. R. Reay, and G. Kovacs “An unconditionally stable two-stage CMOS amplifier”, *IEEE J. of Solid-State Circuits*, vol. 30, no. 5, pp. 591-594, May 1995.
50. B. Ahuja, “An improved frequency compensation technique for CMOS operational amplifiers”, *IEEE J. Solid-State Circuits*, vol. SC-18, no. 12, pp. 629-633, Dec. 1983.
51. V. Ivanov, “CMOS input stage with wide common-mode range”, US pat. 6,509,795, 2003.
52. R. Griffith, R. Vyne, R. Dotson, and T. Petty, “A 1V BiCMOS rail-to-rail amplifier with n-channel depletion-mode input stage”, *ISSCC-1997Digest Tech. Papers*, pp. 352-353, 484, Feb. 6-8, San Francisco, 1997.
53. R. Blauschild, “Differential amplifier with rail-to-rail capability”, US pat. 4,532,479, 1985.
54. R. Burt, private communication.
55. *OPA627 data sheet and application notes*, *www.ti.com*.
56. S. Zhang, and V. Ivanov, “Rail-to-rail CMOS input stage of the operational amplifier with constant transconductance” US pat. 6,462,619.
57. *OPA277 data sheet and application notes*, *www.ti.com*.
58. V. Ivanov, J. Zhou, and W. Meinel, “Operational amplifier input stage and method”, US pat. 6,642,789, 2003.
59. *OPA725 data sheet and application notes*, *www.ti.com*.
60. A. Tang, “Bandpass spread spectrum clocking for reduced clock spurs in autozeroed amplifiers”, *Proc. ISCAS-2001*, vol. 1, pp. 663-666, May 6-9, Sidney, 2001.

61. T. Stockstad, and H. Yoshizawa, “A 0.9 V 0.5 uA rail-to-rail CMOS OpAmp”, *IEEE J. Solid-State Circuits*, vol. 37, no. 3, pp. 286-292, March 2002.
62. V. Ivanov, J. Zhou, and W. Meinel, “Method and circuit for trimming offset and temperature drift for operational amplifiers and voltage references”, US pat. 6,628,169, 2003.
63. A. Wang et al., “A Mixed-mode ESD protection circuit simulation-design methodology”, *IEEE J. Solid-State Circuits*, vol. 38, no. 6, pp. 995-1006, 2003.
64. Y. Tsividis, *Operation and modeling of MOS transistor*, New York: McGraw-Hill, 1987.
65. V. Ivanov, “Rail-to-rail input/output operational amplifier and method”, US pat. 6,150,883, 2000.
66. R. Wassenaar et al., “Design aspects of rail to rail CMOS OpAmp”, Proceedings of the 1st VLSI Workshop, pp. 23-28, Columbus OH, May 1997.
67. G. Johnson, and V. Ivanov, “Rail-to-rail input/output operational amplifier and method”, US pat. 6,356,153, 2002.
68. S. Sanchez, V. Ivanov, and W. Meinel, “Amplifier gain boost circuitry and method”, US pat. Application, 2003.
70. J. Ramirez-Anguilo et al., “The flipped voltage follower: a useful cell for low-voltage low-power circuit design”, *Proc. ISCAS-2002*, vol. 3, pp. 26-29, Phoenix AZ, May 26-29, 2002.
71. E. Vittoz, “Low-power low-voltage limitations and prospects in analog design” in *Low-power Low-voltage Integrated filters and Smart Power*, Dordrecht, The Netherlands: Kluwer, 1994
72. D. Monticelli, “Class AB output circuit with large swing”, US pat. 4,570,128, 1986.
73. G. Erdi, “A Precision Trim Technique for Monolithic Analog Circuits”, *IEEE J. Solid-State Circuits*, vol. SC-1, no. 6, pp. 412-416, Dec. 1975.
74. J. Price, “Programmable circuit”, US pat. 3,191,151, 1962.
75. M. Cohen, B. Unger, and J. Milkosky, "Laser machining of thin films and integrated circuits", Bell Syst. Tech. Journal., vol. 47, pp. 385-405, 1968.
76. E. Swenson, “The evolution of laser processing in semiconductor manufacturing”, *Proc. 26th Midwest Symp. Circuits and Systems*, p. 212, Puebla, Mexico, Aug. 15-16, 1983.
77. A. Sypherd, and N. Solman, “Automatic laser encoding of semiconductor ROM”, *Proc. National Electronic Conference*, pp. 206-209, Dec. 9-11, Chicago, IL, 1968.
78. G. Chaplin, and A. Owens, "Some transistor input stages for high-gain d.c. amplifiers", Proc. IEE, Part B, No. 21, pp. 249-257, May 1958.
79. F. Goodenough, “Rail-to-Rail Op Amps Use Depletion-Mode PMOSFETs”, *Electronic Design*, p. 127, Apr. 16, 1992.
80. J. Fonderie, and J. Huijsing “Operational amplifier with 1V rail-to-rail multipath-driven output stage”, *IEEE J. Solid-State Circuits*, vol. 26, no. 12, pp. 1817-1824, Dec. 1991.
81. V. Ivanov, “Push-pull stage of the operational amplifier”, US pat. 5,973,564, 1998.
82. P. Bruschi, D. Navarrini, and M. Piotto, “A high current drive CMOS output stage with tunable quiescent current limiting circuit”, *IEEE J. Solid-State Circuits*, vol. 38, no. 8, pp. 1416-1420, Aug. 2003.
83. E. Seevinck, *Analysis and synthesis of translinear integrated circuits*, PhD Thesis, University of Pretoria, 1981.
84. R. R. Troutman, *Latchup in CMOS technology : the problem and its cure*, Dordrecht, The Netherlands: Kluwer, 1986.
85. V. Ivanov, “Fast rail-to-rail class AB output stage having stable output bias current and linear performance”, US pat. 6,366,169, 2002.
86. *OPA349 data sheet and application notes*, *www.ti.com*.

87. *OPA379 data sheet and application notes*, *www.ti.com*.
88. *OPA244 data sheet and application notes*, *www.ti.com*.
89. C. Enz, and G. Temes, "Circuit techniques for reducing the OpAmp imperfections: autozeroing, correlated double sampling and chopper stabilization", *Proc. IEEE*, vol. 84, no. 11, pp. 1584-1614, 1996.
90. G. Erdi, "Common-mode rejection in monolithic operational amplifiers", *IEEE J. Solid-State Circuits*, vol. SC-5, no. 6, pp. 365-367, 1970.
91. *REF31xx data sheet and application notes*, *www.ti.com*.
92. Е. Попов, *Теория линейных систем автоматического управления и регулирования*, Москва: Наука, 1989, (E. Popov, *Linear control system theory,* Moscow, Nauka Pub. House, 1989, in Russian).
93. I. Horowitz, *Synthesis of feedback systems*, London, England: Academic Press Inc.: 1963.
94. S. Mason, and H. Zimmermann, *Electronic circuits, signals and systems*, New York: Wiley, 1960.
95. S. Zhang, and V. Ivanov, "Quick turn-on enable/disable bias control circuit", US pat. 6,400,207, 2002.
96. R. Widlar, and M. Yamatake, "Dynamic safe-area protection for power transistors employs peak-temperature limiting", *IEEE J. Solid-State Circuits*, vol. 22, no. 1, pp. 77-84, Feb. 1987.
97. R. Widlar, and M. Yamatake, "A monolithic power op amp", *IEEE J. Solid-State Circuits*, vol. 23, no. 2, pp. 527 –535, April 1988.
98. B. Murari, "Power Integrated Circuits: Problems, Tradeoffs, Solutions", *IEEE J. Solid-State Circuits*, vol. 13, no. 3, 1978.
99. D. Baum, and V. Ivanov, "Overcurrent protection circuit and method", US pat. Application, 2002.
100. M. Ivanov, *Low-Voltage Low-Power CMOS Operational Amplifier Stages with Class AB common-mode feedback,* MSEE thesis, Ohio State University, Columbus, 1997.
101. D. Baum, and V. Ivanov, "Slew rate boost circuit and method", US pat. 6,437,645, 2002.
102. S. Zhang, G. Johnson and V. Ivanov, "Slew rate boost circuit and method", US pat. 6,359,512, 2002.
103. B. Carter, "Video multiplexer uses high-speed op amps", *EDN*, 8/21, p. 87, 2003.
104. S. Zhang, and V. Ivanov, "Overload recovery circuit and method", US pat. 6,317,000, 2001.
105. *OPA355 data sheet and application notes*, *www.ti.com*.
106. P. Brokaw, "Bandgap reference design", MEAD Microelectronics Class on Power Management, Lausanne, 2003.
107. J. Haslett, "Noise performance of new Norton OpAmps", *IEEE Trans. Electronic Devices*, vol. 21, pp. 571-577, Sept. 1974.
108. B. Razavi, *Design of Analog CMOS Integrated Circuits*, New York: McGraw Hill, 2001.
109. I. Filanovsky, and L. Najafizadeh "Zeroing in On a Zero-Temperature Coefficient Point", *Proc. IEEE 45th Int. Midwest Symp. Circuits and Systems*, vol. 1, pp. 271-274, Tulsa, OK, Aug. 2002.
110. J. Solomon, "The monolithic Op Amp: a tutorial study", *IEEE J. Solid-State Circuits*, vol. 9, no. 12, pp. 314-332, Dec. 1974.
111. *Low-voltage design for portable systems*, Special Topic Evening Session, *ISSCC-2002*, Feb. 3-7, San Francisco, 2002.
112. H. Gummel, and H. Poon, "An integral charge control models of bipolar transistors", *Bell Systems Technical Journal*, vol. 49, pp 827-852, 1970.
113. *HSPICE user's manual*, Meta-Software, Inc., 2000.

114. D. Foty, *MOSFET Modeling with SPICE: Principles and Practice*, Upper Saddle River, NJ: Prentice-Hall, 1997.
115. J. F. Dickson, “On-chip high-voltage generation in NMOS integrated circuits using an improved voltage multiplier technique”, *IEEE J. Solid-State Circuits*, vol. 11, pp. 374–378, June 1976.
116. G. Palmisano, G. Palumbo, and G. Pennisi, “Harmonic distortions in class AB output stages”, *IEEE Trans. Circuits and Systems*, Part II, vol. 45, no. 2, pp. 243-250, Feb. 1998.
117. F. You et al., “Low-voltage class AB buffers with quiescent current control”, *IEEE J. Solid-State Circuits*, vol. 33, no. 6, pp. 915-920, Jun. 1998.
118. V. Ivanov, “Class AB output stage with stable quiescent current”, US pat. Application, 2003.
119. R.M. Fox, "Design-oriented analysis of DC operating-point instability", *Proc. ISCAS-1995*, vol. 1, pp. 109-112, May 1995.
120. R.M. Fox, "A general operating-point instability test based on feedback analysis", *Proc. ISCAS-1998,* v.3, pp. 550-553, Orlando FL, May-June 1998

Index